A Multi-state Physics Model of Component Degradation based on Stochastic Petri Nets and Simulation

Yan-Fu Li, Enrico Zio, Yan-Hui Lin

A Multi-state Physics Model of Component Degradation based on Stochastic Petri Nets and Simulation

Y.F. Li[1] member IEEE, E. Zio[1,2] senior member IEEE, Y.H. Lin[1]

[1] *Chair on Systems Science and the Energetic Challenge, European Foundation for New Energy-Electricite' de France, at Ecole Centrale Paris- Supelec, France*

yanfu.li@ecp.fr, yanfu.li@supelec.fr, enrico.zio@ecp.fr, enrico.zio@supelec.fr

[2]*Politecnico di Milano, Italy*

enrico.zio@polimi.it

Abstract - Multi-state physics modeling (MSPM) of degradation processes is an approach proposed for estimating the failure probability of components and systems. This approach integrates multi-state modeling, which describes the degradation process through transitions among discrete states (e.g. initial, micro-crack, rupture, etc), and physics modeling by (physics) equations that describe the degradation process within the states. In reality, the degradation process is non-Markovian, its transition rates are time-dependent, and the degradation is possibly influenced by uncertain external factors such as temperature and stress. Under these conditions, it is in general difficult to derive the state probabilities analytically.
In this paper, we overcome this difficulty by building a simulation model supported by a stochastic Petri net representing the multi-state degradation process. The proposed modeling approach is applied to the problem of a nuclear component undergoing stress corrosion cracking. The results are compared with those derived from the state-space enrichment Markov chain approximation method applied in a previous work of literature.

Keywords – Component degradation, multi-state physics model, non-homogeneous Markov process, Monte Carlo simulation, stochastic Petri net.

Acronyms

CDF	Cumulative distribution function
CTMC	Continuous time Markov chain
DTMC	Discrete time Markov chain
MC	Monte Carlo
MSM	Multi-state model
MSPM	Multi-state physics model
NHCTMM	Non-homogenous continuous time Markov model
PDF	Probability density function

PN	Petri-net
SPN	Stochastic Petri net

Notations

$\boldsymbol{S}$	The vector of component degradation states
$\boldsymbol{S}_e$	The vector of enriched state space considering process holding time
t	Time
$\emptyset(t)$	The discrete function representing the stochastic degradation process, which takes values from $\boldsymbol{S}$
$M+1$	The total number of component degradation states
$\boldsymbol{P}(t)$	The vector of component state probability at time *t*
$\lambda_{i,j}(t,\boldsymbol{\theta})$	The transition rate from state *i* to state *j* at time *t*, given the realizations of the uncertain external influencing factors $\boldsymbol{\theta}$
$\boldsymbol{\theta}=\{\theta_0,\dots,\theta_N\}$	The vector of uncertain external influencing factors, where *N*+1 is the total number of factors
$p(\boldsymbol{\theta})$	Probability density function of $\boldsymbol{\theta}$
p_i^{PN}	Place *i* of the Petri nets
t_j^{PN}	Transition *j* of the Petri nets
Δt_i	The holding time at state *i*
$F(t\|t',\boldsymbol{\theta})$	Cumulative distribution function of holding time Δt_i given $\boldsymbol{\theta}$
$q_{i,j}(t\|\boldsymbol{\theta})$	The transition probability from state *i* to state *j* at time *t* given $\boldsymbol{\theta}$

1. Introduction

Most products, components, and systems age, wear, and degrade over time until they are completely failed or exhausted. Degradation processes have been intensively studied by the reliability engineering community [1]-[10]. In general, the degradation models can be classified into analytical models [3], [7]-[10], and simulation models [5]-[6], [11]. The analytical degradation models can be further classified into the following three groups.

1. Statistical models of time to failure (e.g. lifetime distribution [7]).
2. Models describing the evolution of a measurable quantity indicating time-dependent degradation, and failure upon reaching a threshold value (e.g. Brownian motion [9], and gamma process [8]).
3. Multi-state models of degradation [3], [10].

Multi-state models (MSM) [12]-[13] are frequently applied for component degradation process modeling because they fit practically to component aging processes in real life situations when there is a range of levels from perfect functioning to complete

failure. To model the dynamics of the degradation process, Markov [14]-[15] and semi-Markov models [16]-[17] have been used. In the Markov models, the transition rates between states are constant, and the state holding times follow exponential distributions, which means that the degradation process is memoryless. In the semi-Markov models, the state holding times may follow arbitrary distributions. In some recent works [18]-[19], the non-homogenous continuous time Markov model (NHCTMM) has been introduced to account for the aging effects of un-repairable components or systems. The component degradation process is also possibly affected by other external factors (e.g. temperature, stress) [20].

Multi-state modeling requires estimating the transition rates from field data. In practice, it can be difficult or even impossible to collect relevant data, especially for the highly reliable devices (e.g. nuclear components, aerospace devices, etc).

To overcome some of the problems mentioned above, a novel approach based on multi-state physics modeling has been proposed [21], in which the transition rates are described by physics functions (e.g. crack growth) rather than estimated from service data. The resulting model is non-Markovian because the transition rates are time-dependent and uncertain. To solve the problem, in the original work by [21], a state-space enrichment approach has been used upon discretization of the component lifetime into equally sized time intervals, during each of which the transition rate remains constant. Then, the component degradation process is converted into a discrete time Markov chain (DTMC) residing in a largely enriched state space described by a tuple $\boldsymbol{S}_e = (\boldsymbol{S}, \boldsymbol{t}_c)$, where $\boldsymbol{S}$ is the vector of original component degradation states, and $\boldsymbol{t}_c$ is the vector of discretized holding times at each state.

In this work, we propose an integrated simulation framework for modeling the stochastic aging behavior of components. Such framework is supported by a stochastic Petri net (SPN), which provides a flexible model representation scheme for describing the state transition process. Uncertain external influencing factors (e.g. temperature, stress) are included. A Monte Carlo (MC) simulation algorithm is proposed to realize the degradation transition process, and compute the state probability distributions.

The rest of the paper is organized as follows. Section 2 presents the formal definition of the multi-state physics model, with consideration of time-dependent transition rates,

and uncertain external influencing factors. Section 3 introduces the stochastic Petri nets. Section 4 presents the integrated framework, and the detailed MC simulation procedures of the integrated model. In Section 5, the real-world case study from Unwin et al. [21]is used as an application, and a comparison is made with the state-space enrichment technique. Section 6 concludes the work, and points out possible future extensions.

2. Multi-state physics modeling of component degradation process

Under the framework of multi-state modeling, the dynamics of component degradation is described by transitions among a finite number of discrete degradation states $\boldsymbol{S} = \{s_0, s_1, \dots, s_M\}$. The solution of the multi-state model is the state probability vector at any time instant t, $\boldsymbol{P}(t) = \{p_0(t), p_1(t), \dots, p_M(t)\}$, given the transition rates $\lambda_{i,j}$ from state i to state j. In the MSPM, the transition rate $\lambda_{i,j}(t, \boldsymbol{\theta})$ is a function of time t, for given values of physical factors $\boldsymbol{\theta}$. This function can be formulated based upon material science knowledge about the degradation physics of the component (e.g. the crack development process [20]). With the consideration of degradation physics, the following assumptions are made for MSPM.

1. The component consists of (M+1) states where states '0,' and 'M' represent the complete failure state, and perfect functioning state, respectively. The generic intermediate state i ($0<i<M$) is a degradation state where the component is partially functioning.
2. The initial state (at time $t = 0$) of the component is M.
3. Repair can be performed on the intermediate states. Once the component is in complete failure (e.g. rupture), it is no longer repairable.
4. The transition rates $\lambda_{i,j}(t, \boldsymbol{\theta})$ from state i to state j is a function of time, and of the external influencing factors $\boldsymbol{\theta}$, whose values may not be precisely known.

Fig. 1 depicts the state-space diagram of the component degradation process with repairs.

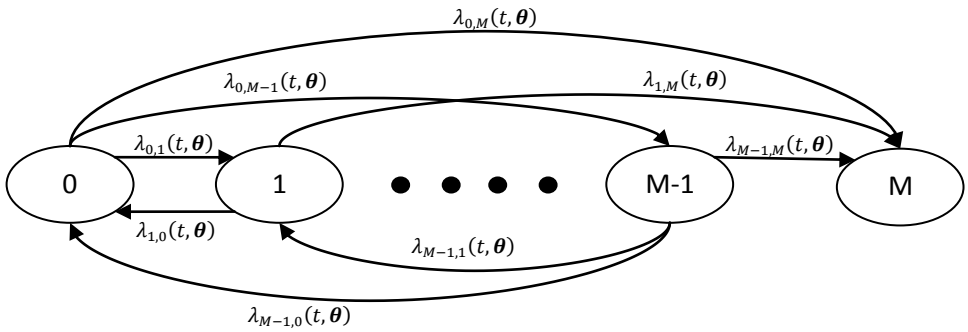

Fig 1. A State-space diagram of the component degradation process.

The transition rate is defined as

$$\lambda_{i,j}(t,\boldsymbol{\theta}) = \lim_{\Delta t \to 0} \frac{\Pr\left(\emptyset(t+\Delta t)=j \mid \emptyset(t)=i, \boldsymbol{\theta}\right)}{\Delta t} \tag{1}$$

where $\boldsymbol{\theta}$ and $\emptyset(t)$ are defined in the notation list and $p(\boldsymbol{\theta})$ is the probability density function (PDF) of $\boldsymbol{\theta}$.

The target of multi-state modeling is to solve the state probability vector $\boldsymbol{P}(t) = \{p_0(t), p_1(t), \dots, p_M(t)\}$ with

$$p_i(t) = \int \Pr(\emptyset(t) = i|\boldsymbol{\theta})\, p(\boldsymbol{\theta}) d\boldsymbol{\theta}. \tag{2}$$

The integral at the right-hand side of (2) is over all possible values of $\boldsymbol{\theta}$. If the transition rates are constant, the state probabilities can be obtained by solving the ordinary differential equations corresponding to the state space diagram.

Solving analytically the Markov model with time-dependent transition rates and possibly random $\boldsymbol{\theta}$ is a difficult task [22]. Then, approximation methods are introduced. One used by several researchers [21]-[22] amounts to discretizing the component lifetime into intervals, and assuming a constant value of transition rate in each interval. By doing so, the description of the stochastic process is converted into a discrete time Markov chain (DTMC) with a significantly enriched state space which includes discrete time steps, and characterized by a sparse transition matrix. For example, given a component

with 6 original degradation states, and a lifetime of 100 years discretized in time steps of 0.5 years, the approximation method would generate a transition matrix of $(6 \times 200)^2$ entries. Alternatively, the simulation modeling framework offers a promising alternative.

3. Stochastic Petri nets

Petri nets (PNs), coined by Carl Petri [23], are an adaptive, versatile, and yet simple graphical modeling tool for representing dynamic systems. PNs have successful applications in the reliability modeling of various systems, such as computer software and hardware systems [24], manufacturing systems [5], occupant safety systems [25], and others.

A PN is a bipartite directed graph with two types of nodes in which abstract objects (tokens), drawn as bold-faced dots, are moved, created, or removed [26]. The two types of nodes are places (states) $p_i^{PN}(i = 0, \dots, M)$, which are circular, and usually denote the states of the system being modeled; and transitions $t_j^{PN}(j = 1, \dots, N)$, which are bars, and denote the transitions corresponding to actions or events that result to a state change. Places are linked only to transitions using directed arcs $a_{p_i^{PN} t_j^{PN}}$, and vice versa. It is possible for a place to have multiple arcs to or from the transition, which can be condensed down to a single arc with a weight or multiplicity denoted by a slash through the arc with a number next to it. If there is no slash, the weight is usually assumed to be 1 (it is also the default weight value).

The tokens, which represent objects in the model, are stored in places. The movements of the tokens passing between places represent the transitions in the system. The transition t_j^{PN} is enabled only if the weight of each incoming arc is at most equal to the number of tokens at the corresponding input place. In original PNs, the transitions are assumed to be immediate. In stochastic PNs (SPNs) a transition can be immediate (in this work, it is noted by a solid bar), deterministically time-delayed, or randomly time-delayed based on a pre-defined probability distribution. Once the time delay has passed, and if transition remains enabled the switching takes place. The switching will remove the number of tokens in each input place corresponding to the weight of the relevant incoming arcs, and create the number of tokens in each output place corresponding to the

weights of the relevant outgoing arcs. More details about the different types of SPNs can be found in [27].

The SPN is often used as a model representation tool. It can be internally converted to a continuous time Markov chain (CTMC), when the time delay at each transition follows an exponential distribution [28]; the Monte Carlo (MC) simulation is used to solve the SPN directly, when time delays are random [29]. For the MSPM formulation embraced in this study of a stochastic degradation process, MC simulation is used to solve the SPN.

4. The Integrated Simulation Model for Component Degradation

4.1. The integration of stochastic Petri nets and uncertain external influencing factors

A graphical sketch of the integration of SPN and uncertain external influencing factors is given in Fig 2. The transition rates are physically dependent on the values of $\boldsymbol{\theta}$, which is a vector of *n* random parameters with joint probability distribution $p(\boldsymbol{\theta})$.

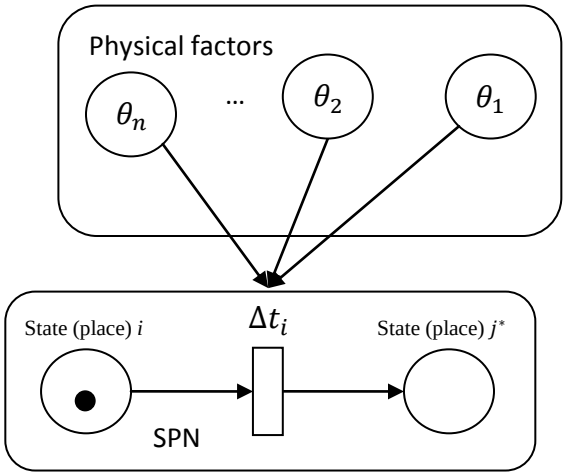

Fig 2. Sketch of the integrated model.

Given the general form of the transition rate (1), the total rate of departure from state *i* is

$$\lambda_i(t, \boldsymbol{\theta}) = \sum_{\substack{j=0 \\ j \neq i}}^{M} \lambda_{i,j}(t, \boldsymbol{\theta}). \quad (3)$$

4.2. Basics of the Monte Carlo simulation model

To obtain the state probability in (2), the following M differential equations need to be solved given the realizations of $\boldsymbol{\theta}$ (the detailed theoretical analysis for Monte Carlo simulation for ICTMC can be found in [30]).

$$\frac{d}{dt}p_i(t|\boldsymbol{\theta}) = \sum_{\substack{k=0 \\ k\neq i}}^{M} p_k(t|\boldsymbol{\theta})q_{k,i}(t|\boldsymbol{\theta})\lambda_k(t,\boldsymbol{\theta}) - p_i(t|\boldsymbol{\theta})\lambda_i(t,\boldsymbol{\theta}) \tag{4}$$

where $i = 1, \dots, M$, and

$$q_{k,i}(t|\boldsymbol{\theta}) = \lambda_{k,i}(t,\boldsymbol{\theta})/\lambda_k(t,\boldsymbol{\theta}). \tag{5}$$

The quantity $q_{j,i}(t|\boldsymbol{\theta})$ is regarded as the conditional probability that, given the transition out of state *j* at time *t*, and the values of $\boldsymbol{\theta}$, the transition arrival state will be i. To rewrite (4) into integral form, an integrating factor $M_i(t,\boldsymbol{\theta}) = \exp\left[\int_0^t \lambda_i(t',\boldsymbol{\theta})dt'\right]$ is used. Multiplying both sides of (4) by the integrating factor, we obtain

$$\frac{d}{dt}\left[p_i(t|\boldsymbol{\theta})M_i(t,\boldsymbol{\theta})\right] = M_i(t,\boldsymbol{\theta})\sum_{\substack{k=0 \\ k\neq i}}^{M} p_k(t|\boldsymbol{\theta})q_{ki}(t|\boldsymbol{\theta})\lambda_k(t,\boldsymbol{\theta}). \tag{6}$$

Taking the integral of both sides, we obtain

$$p_i(t)M_i(t,\boldsymbol{\theta}) = p_i(0) + \int_0^t \left[M_i(t',\boldsymbol{\theta})\sum_{\substack{k=0 \\ k\neq i}}^{M} p_k(t'|\boldsymbol{\theta})q_{ki}(t'|\boldsymbol{\theta})\lambda_k(t',\boldsymbol{\theta})\right]dt'. \tag{7}$$

Substituting $M_i(t,\boldsymbol{\theta})$ with $\exp\left[\int_0^t \lambda_i(t',\boldsymbol{\theta})dt'\right]$, we obtain

$$p_i(t|\boldsymbol{\theta}) = p_i(0)\exp\left[-\int_0^t \lambda_i(t',\boldsymbol{\theta})dt'\right] +$$

$$\int_0^t \exp\left[-\int_{t'}^t \lambda_i(t'',\boldsymbol{\theta})dt''\right]\sum_{\substack{k=0 \\ k\neq i}}^{M} p_k(t'|\boldsymbol{\theta})q_{ki}(t'|\boldsymbol{\theta})\lambda_k(t',\boldsymbol{\theta})\,dt'. \tag{8}$$

In the MC simulation, the probability distribution function $p_i(t|\boldsymbol{\theta})$ is not sampled directly. Instead, the process holding time at state *i* is sampled, and then the transition from state *i* to another state *j* is determined. This procedure is repeated until the accumulated holding time reaches the predefined time horizon. The resultant time sequence consists of the holding times at different states.

To sample the holding time, the probability density (or total frequency) of the departing state *i*, $\psi_i(t|\boldsymbol{\theta})$, needs first to be obtained by multiplying $\lambda_i(t,\boldsymbol{\theta})$ to both sides of (8).

$$\psi_i(t|\boldsymbol{\theta}) = \lambda_i(t,\boldsymbol{\theta})p_i(t|\boldsymbol{\theta})$$

$$= p_i(0)\cdot\lambda_i(t,\boldsymbol{\theta})\cdot\exp\left[-\int_0^t \lambda_i(t',\boldsymbol{\theta})dt'\right] + \int_0^t \lambda_i(t,\boldsymbol{\theta})\cdot\exp\left[-\int_{t'}^t \lambda_i(t'',\boldsymbol{\theta})dt''\right]\cdot\sum_{\substack{k=0\\k\neq i}}^{M}\psi_k(t'|\boldsymbol{\theta})q_{ki}(t'|\boldsymbol{\theta})\,dt'$$

$$= p_i(0)f_i(t|0,\boldsymbol{\theta}) + \sum_{\substack{k=0\\k\neq i}}^{M}\int_0^t \psi_k(t'|\boldsymbol{\theta})q_{ki}(t'|\boldsymbol{\theta})f_i(t|t',|\boldsymbol{\theta})dt' \qquad (9)$$

where

$$f_i(t|t',\boldsymbol{\theta}) = \lambda_i(t,\boldsymbol{\theta})\exp\left[-\int_{t'}^t \lambda_i(t'',\boldsymbol{\theta})dt''\right] \qquad t \geq t'. \qquad (10)$$

This result is defined as the conditional probability density function (PDF) that the process will depart state *i* at time *t*, given that the process is at state *i* at time t', and the values of the external influencing factors $\boldsymbol{\theta}$. Equation (9) indicates that the probability density function $\psi_i(t|\boldsymbol{\theta})$ consists of the sum of contributions from the random walks with transitions passing through all the states (including state *i*) from time 0 to *t*, given the values of $\boldsymbol{\theta}$. To obtain the marginal distribution $\psi_i(t)$, the conditional distribution is multiplied with the PDF of $\boldsymbol{\theta}$, and the result is integrated over all possible values of $\boldsymbol{\theta}$:

$$\psi_i(t) = \int \psi_i(t|\boldsymbol{\theta})\,p(\boldsymbol{\theta})d\boldsymbol{\theta}\,. \qquad (11)$$

Based on (11), the MC simulation procedure mentioned above can be derived. The CDF of the departure time t given that it is at state *i* at time t' is denoted as

$$F_i(t|t') = \int F_i(t|t',\boldsymbol{\theta})p(\boldsymbol{\theta})d\boldsymbol{\theta} = 1 - \int \exp\left[-\int_{t'}^t \lambda_i(t'',\boldsymbol{\theta})dt''\right]p(\boldsymbol{\theta})d\boldsymbol{\theta}. \qquad (12)$$

Given t', and (12), the departure time t can be sampled through direct inversion sampling, acceptance-rejection sampling, and other sampling techniques [31].

Following the departure, the marginal transition probabilities to any other state $j = \{0, \dots M | j \neq i\}$ are calculated as

$$q_{i,j}(t) = \int \frac{\lambda_{i,j}(t,\boldsymbol{\theta})}{\lambda_i(t,\boldsymbol{\theta})} p(\boldsymbol{\theta}) d\boldsymbol{\theta}, \tag{13}$$

and a uniformly distributed random number U is sampled in the interval [0,1]; if $\sum_{k=0}^{j^*-1} q_{i,k}(t) < U < \sum_{k=0}^{j^*} q_{i,k}(t)$, then the transition to state j^* is activated, and occurs at t units of time. After time $\Delta t_i = t - t'$, a new token will appear at place j^*, and the token at place i is removed.

4.3 The simulation procedures

Prior to the simulation, incorporation of the external influencing factors should be carried out through the following steps.

1) Formulate the functions describing the physics of the transition rates.

2) Identify the external influencing factors θ_i (e.g. temperature, stress).

3) Define the distribution functions, $p(\boldsymbol{\theta})$ representing the uncertainties in the values of these factors.

The algorithm for the simulation of the process of component degradation on the time horizon $[0, t_{max}]$ is sketched in the following pseudo-code.

Initialize the system by allocating a token onto place $i = M$ (initial state of perfect performance), setting the time $t = 0$ (initial time), and setting the total number of replications to N_{max}.
Set $t' = 0$.
Set $n = 1$.
While $n < N_{max}$,
    While $t < t_{max}$,

sample a realization of the external influencing factors $\boldsymbol{\theta}$ from the joint probability function $p(\boldsymbol{\theta})$.

Sample a departure time t from the distribution function $F_i(t|t', \boldsymbol{\theta})$.

Sample a random number U from the uniform distribution in [0, 1].

For each outgoing transition (j = 0,*1*,…,*M*, $j \neq i$),

Calculate the transition probability $q_{i,j}(t, \boldsymbol{\theta})$.

If $\sum_{k=0}^{j^*-1} q_{i,k} < U < \sum_{k=0}^{j^*} q_{i,k}$,

then activate the transition to state j^*.

End If.

End For.

Set $t' = t$.

Remove the token from place *i*, and add a new token onto place j^*.

End While.

Set $n = n + 1$.

End While. □

Subsequent to the execution of the simulation algorithm, an estimate $\widehat{\boldsymbol{P}}(t) = \{\widehat{p_0}(t), \widehat{p_1}(t), \dots, \widehat{p_M}(t)\}$ of the state probability vector is computed by dividing the total number of visits to each state by the total number of simulations N_R : $\widehat{\boldsymbol{P}}(t) = \frac{1}{N_{max}}\{n_0(t), n_1(t), \dots, n_M(t)\}$, where $\{n_i(t)|i = 0, \dots, M, t \leq t_{max}\}$ is the total number of visits to state *i* at time *t*. The derived distributions $p(\boldsymbol{\theta})$ and $F_i(t|t')$ may have complicated mathematical expressions; under these circumstances, the Markov Chain MC technique can be used to sample random values [6].

5. Experiments, and results

5.1 Case study

The case study refers to the cracking process in an Alloy 82/182 dissimilar metal weld in a primary coolant system of a nuclear power plant [21]. Cracks can grow from the inner to the outer diameter of the dissimilar metal welds in one of the three major morphologies: axial, radial, and circumferential. The latter two types can lead to the rupture of the component. The crack growth has two steps 1) crack initiation, and 2) crack propagation.

The radial crack mainly grows outward from the initiation site towards the outer diameter; the process can lead to a leak, and potentially to rupture. The crack grows relatively evenly around the circumference, potentially leading to a rupture.

The Alloy 82/182 crack growth rate equations have been studied by various organizations including Ringhals AB, Electricité de France, and the Electric Power Research Institute. The forms that these equations take are similar, and include a stress and Arrhenius temperature dependence

$$\dot{a} = \frac{da}{dt} = \alpha f_{alloy} f_{orient} K^{\beta} e^{[-(Q/R)(1/T - 1/T_{ref})]} \tag{14}$$

where $\dot{a}$ ($\dot{a} \geq 0$) is the crack growth rate in time, a is the crack length (m), t is the time since crack initiation (s), α is the crack growth amplitude, f_{alloy} is a constant (equal to 1.0, and 0.385 for Alloy 182, and Alloy 82 respectively), f_{orient} is a constant equal to 1.0, K is the crack tip stress intensity factor (MPa√m), β is the stress intensity exponent, Q is the thermal activation energy for crack growth (kJ/mole), R is the universal gas constant (kJ/mole-^{o}K), T is the absolute operating temperature at crack location (^{o}K), and T_{ref} is the absolute reference temperature used to normalize data (^{o}K).

The multi-state physics model, proposed by Unwin et al. [21] to describe the crack growth in the case study of interest, is represented in Fig. 3.

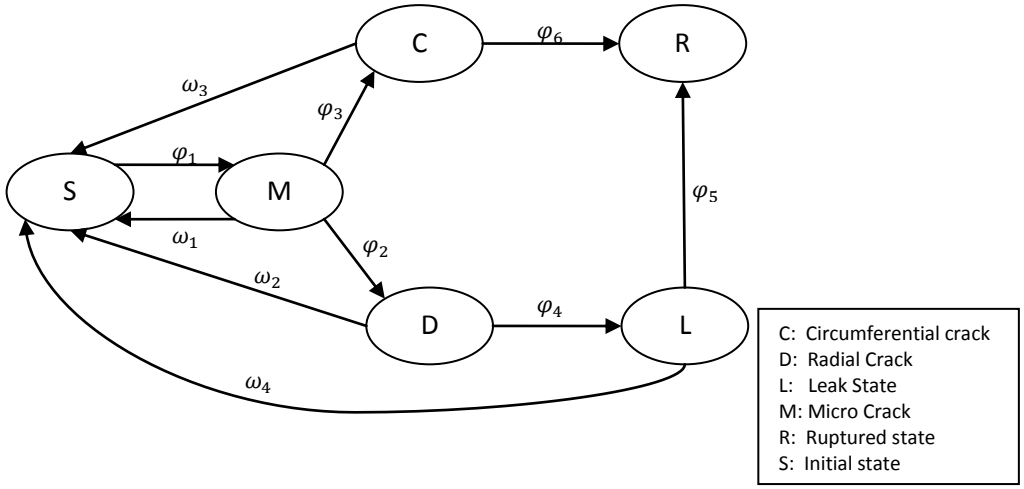

Fig. 3. Transition diagram of the multi-state physics model of crack development in Alloy 82/182 dissimilar metal welds.

In [21], the transition rates φ_1, φ_2, φ_3 , and φ_4 are time-dependent, and stochastic, whereas the others are assumed constant.

The transition rate φ_1 from initial state *S* to micro-crack state *M* is defined as

$$\varphi_1 = \int \left(\frac{b}{\tau}\right) \cdot \left(\frac{t}{\tau}\right)^{b-1} \cdot f_{PDF}(\tau, b)\, d\tau db \tag{15}$$

where $f_{PDF}(\tau, b)$ is the joint probability density function of τ and b, and the integral is defined over the domains of τ and b. τ is a time constant which has been observed to have both a stress and temperature dependence; b is a fitting parameter.

The transition rates φ_2, and φ_3, describing the transitions from micro-crack state *M* to radial-crack state *D*, and circumferential-crack state *C*, respectively, have similar definitions. Let a_D denote the threshold length of a radial-crack; then, at time u after crack initiation, the probability of the state *D* is defined as

$$D(u) = P_D \cdot Pr[a_D \leq \int_0^u \dot{a}(t)dt] \tag{16}$$

where P_D is the probability that the crack grows to state *D* given that the current state is *M*. The analogous probability $C(u)$ that the crack goes to state *C* at time u after crack initiation is defined as

$$C(u) = P_C \cdot Pr[a_C \leq \int_0^u \dot{a}(t)dt] \tag{17}$$

where a_C is the threshold length of a circumferential-crack, and P_C is the probability that the crack goes to state *C* given that the current state is *M*.

The transition rate φ_2 (between state *M* and *D*) is defined as [32]

$$\varphi_2 = \frac{dD(u)/du}{1-D(u)} = \frac{(a_D/u)^2 \cdot \pi(a_D/u) P_D}{1-P_D \int_{a_D/u}^{\infty} \pi(\dot{a}) d\dot{a}}, \tag{18}$$

and similarly,

$$\varphi_3 = \frac{dC(u)/du}{1-C(u)} = \frac{(a_C/u)^2 \cdot \pi(a_C/u) P_C}{1-P_C \int_{a_C/u}^{\infty} \pi(\dot{a}) d\dot{a}}. \tag{19}$$

By assuming that the crack growth rate $\dot{a}$ is following a uniform distribution with a maximum value of $\dot{a}_M$, i.e.

$$\pi(\dot{a}) = \begin{cases} \frac{1}{\dot{a}_M}, & if\ 0 < \dot{a} < \dot{a}_M \\ 0, & else \end{cases}, \tag{20}$$

then (10), and (11) are reduced to

$$\varphi_2 = \begin{cases} \frac{a_D P_D}{\dot{a}_M u^2 (1 - P_D(1 - a_D/(u\dot{a}_M)))}, & if\ u > a_D/\dot{a}_M \\ 0, & else \end{cases}, \tag{21}$$

and

$$\varphi_3 = \begin{cases} \frac{a_C P_C}{\dot{a}_M u^2 (1 - P_C(1 - a_C/(u\dot{a}_M)))}, & if\ u > a_C/\dot{a}_M \\ 0, & else \end{cases} \tag{22}$$

respectively.

The transition rate φ_4 from state *D* to state *L* is defined by the growth in crack size up to a threshold a_L of leakage:

$$L(w) = Pr[a_L - a_D \leq \int_0^w \dot{a}(t)dt] \tag{23}$$

$$\varphi_4 = \frac{dL(w)/dw}{1 - L(w)} \tag{24}$$

where *w* is the time since the radial crack formation [21]. By assuming the same distribution over the crack growth rate, then

$$\varphi_4 = \begin{cases} \frac{1}{w}, & if\ w > (a_L - a_D)/\dot{a}_M \\ 0, & else. \end{cases} \tag{25}$$

Transition rates from leak to rupture, and from circumferential crack to rupture, are assumed to be constant. These transition rates, together with other constant parameters, are presented in Table I below.

Table I
Case Study Parameter Definitions, and Values

b –Weibull shape parameter for crack initiation model	2.0

τ – Weibull scale parameter for crack initiation model	4 years
a_D – Crack length threshold for radial macro-crack	10 mm
P_D – Probability that micro-crack evolves as radial crack	0.009
$\dot{a}_M$ – Maximum credible crack growth rate	9.46 mm/yr
a_C – Crack length threshold for circumferential macro-crack	10 mm
P_C – Probability that micro-crack evolves as circumferential crack	0.001
a_L – Crack length threshold for leak	20 mm
ω_1- Repair transition rate from micro-crack	1 x10-3 /yr
ω_2- Repair transition rate from radial macro-crack	2 x10-2 /yr
ω_3- Repair transition rate from circumferential macro-crack	2 x10-2 /yr
ω_4- Repair transition rate from leak	8 x10-1 /yr
φ_5 – Leak to rupture transition rate	2x10-2 /yr
φ_6 – Macro-crack to rupture transition rate	1x10-5 /yr

5.2 Results

The simulation model supported by a Petri net description of the degradation process (Fig. 4) is applied to the case study with the parameter settings reported in Table I. In the original study [21], the uncertainties of the external influencing factors (e.g. temperature and pressure) have not been modeled in the crack initiation process (as shown in (15)), and have been implicitly modeled in the crack propagation process by means of a uniform distribution of the transition rate $\dot{a}_M$ (as shown in(20)).

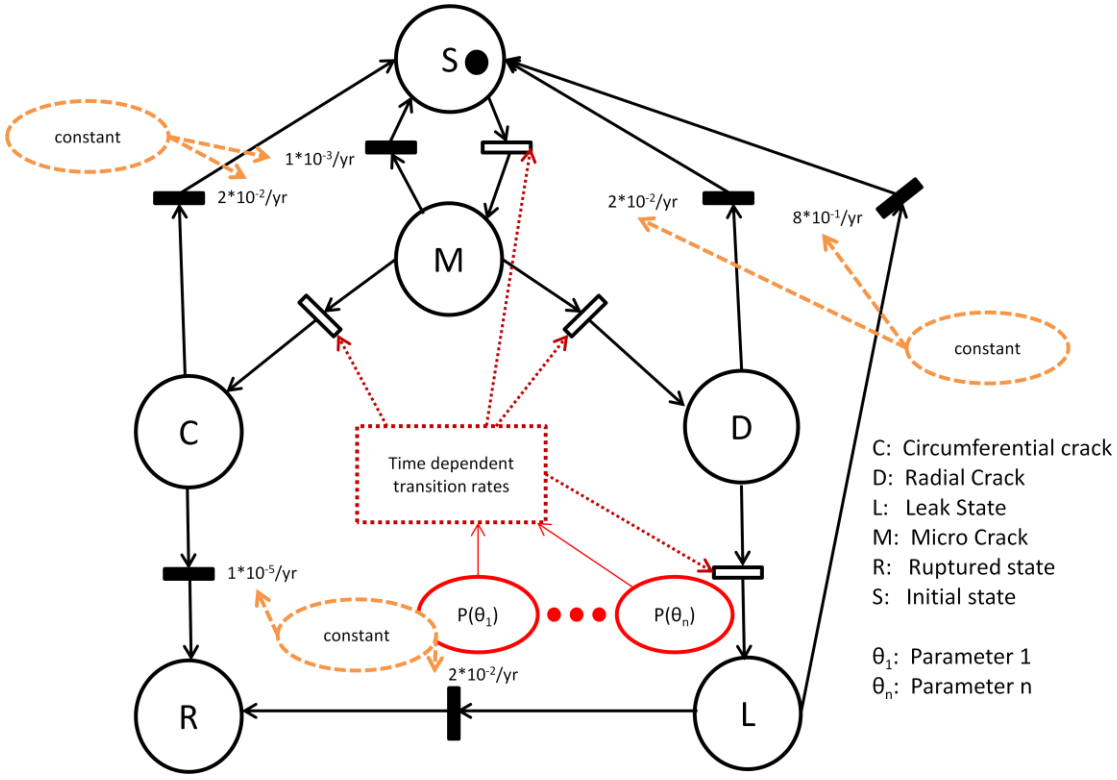

Fig 4. The SPN simulation model of Alloy 82/182 dissimilar metal weld degradation.

The simulation model has been executed $N_{max} = 10^7$ times over a component lifetime $t_{max} = 80$ years, in line with the original study. To investigate the convergence of the simulation model, the 10^7 realizations have been subdivided into N = 20 subsamples of 500,000 each. The sample mean and variance of the estimated state probabilities are calculated as

$$\overline{\boldsymbol{P}}(t) = \frac{1}{N}\sum_{k=1}^{N} \widehat{\boldsymbol{P}}(t)_k \tag{26}$$

$$var_{\widehat{\boldsymbol{P}}(t)} = \frac{1}{N-1}\sum_{k=1}^{N}\left[\widehat{\boldsymbol{P}}(t)_k - \overline{\boldsymbol{P}}(t)\right]^2 \tag{27}$$

where $\widehat{\boldsymbol{P}}(t)_k$ is the estimated state probability vector from the k-th subsample. The convergence of the state probability values can be observed by the variance in (27), and the sequence of sample means on the steadily incremental subsamples

$$\boldsymbol{P}(t)_{conv,k} = \frac{1}{n}\sum_{k=1}^{n} \widehat{\boldsymbol{P}}(t)_k \tag{28}$$

where n takes value from 1 to N.

At t = 80 years, the variances are 0.6749×10^{-8}, 0.776×10^{-8}, 0.0352×10^{-8}, 0.0106×10^{-8}, 0.0037×10^{-8}, and 0.0337×10^{-8} for 'initial', 'micro-crack', 'circumferential', 'radial', 'leak', and 'rupture' states, respectively. Similar results are found at different time moments. The examples of convergence curves at 80 years are presented in Fig. 5. The good stabilization of $\boldsymbol{P}(80)_{conv,k}$ is manifested. It is also noted that $\boldsymbol{P}(t)_{conv,k} = \overline{\boldsymbol{P}}(t)$. Similar convergence curves are obtained at different time moments, but are not presented to save space.

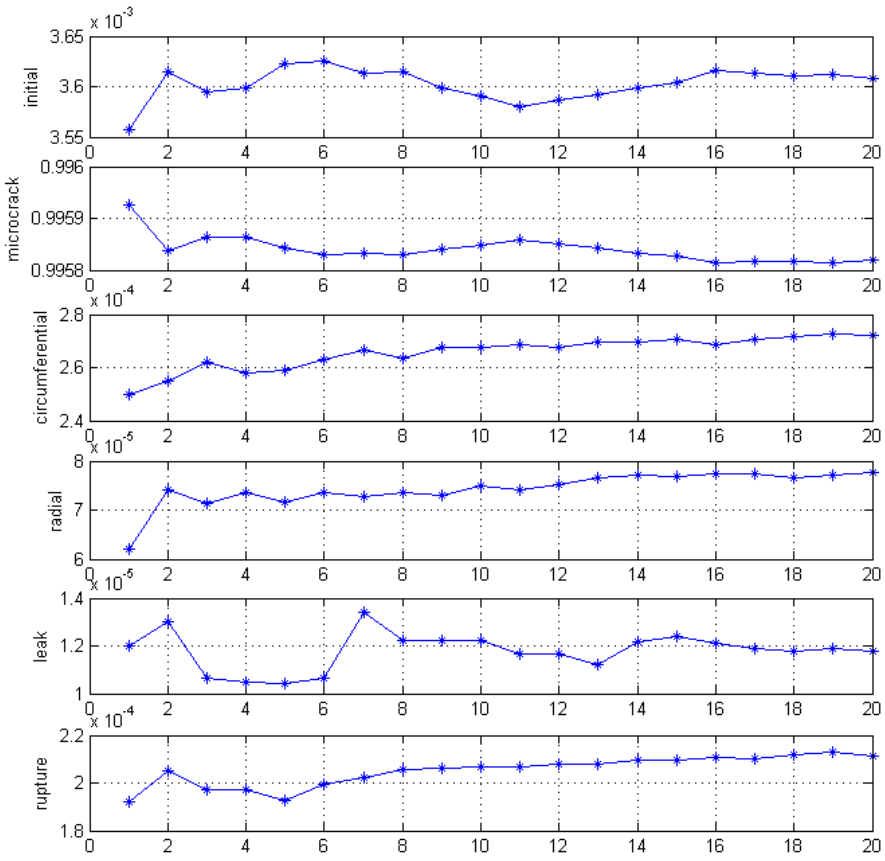

Fig 5. Convergence plots of state probabilities at t = 80 years.

For comparison with the state-space enrichment technique proposed in the original study of [21], the state probabilities resulting from 10^7 simulation runs are shown in Fig. 6 as functions of time. The results from the state-space enrichment method considering different step sizes (e.g. 1 year, 0.5 year, and 0.1 year) are shown in Figs. 7 to 9, respectively. The general shapes and trends of the results are similar for the simulation , and the state-space enrichment with different steps; in all plots, there is: 1) an early, rapid transition from the Initial state to the Micro-crack state; 2) a monotonic increase in the probability of the rupture state.

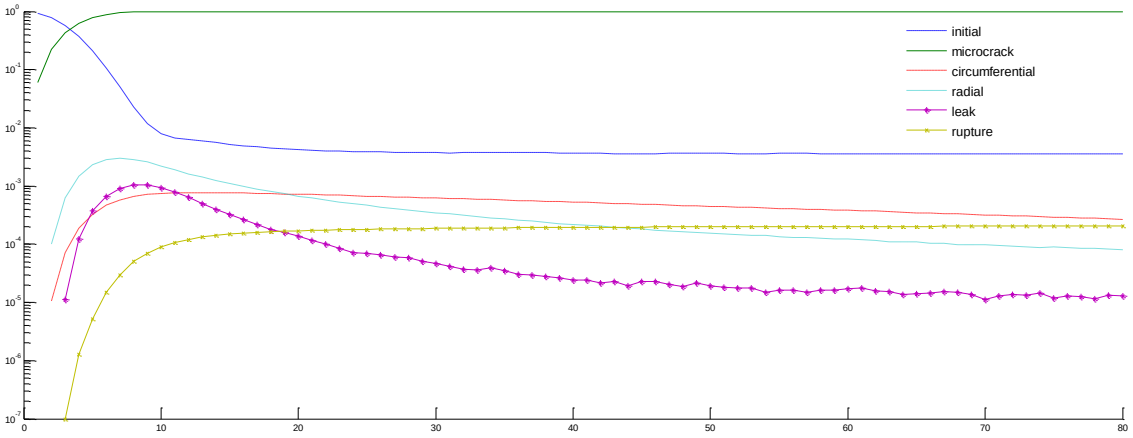

Fig 6. State probabilities obtained by simulation.

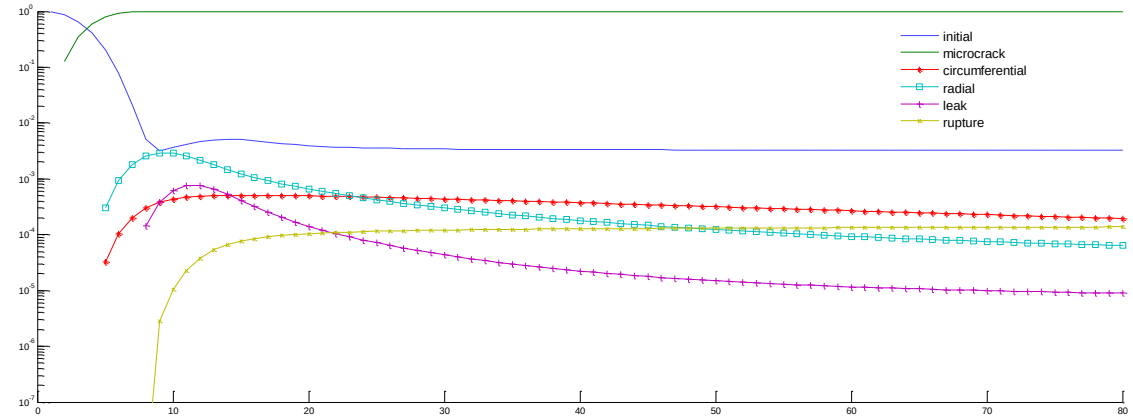

Fig 7. State probabilities obtained by state-space enrichment with step size = 1 year.

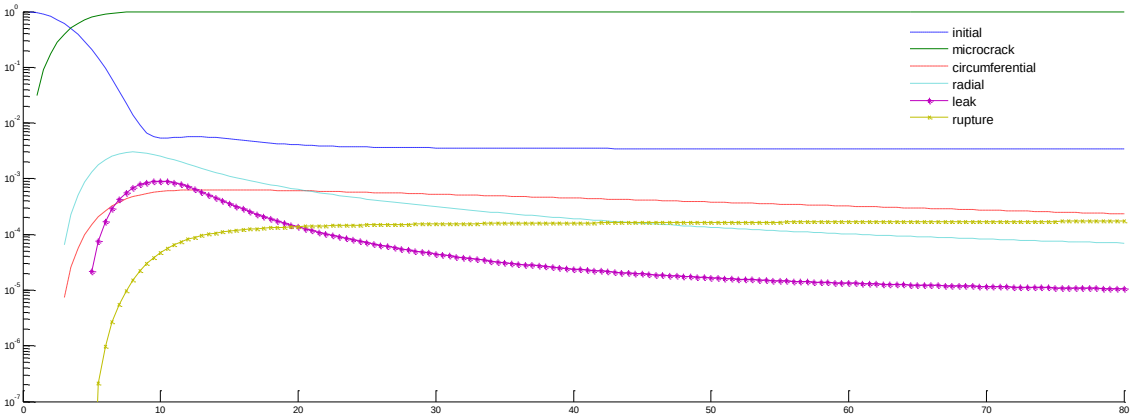

Fig 8. State probabilities obtained by state-space enrichment with step size = 0.5 year

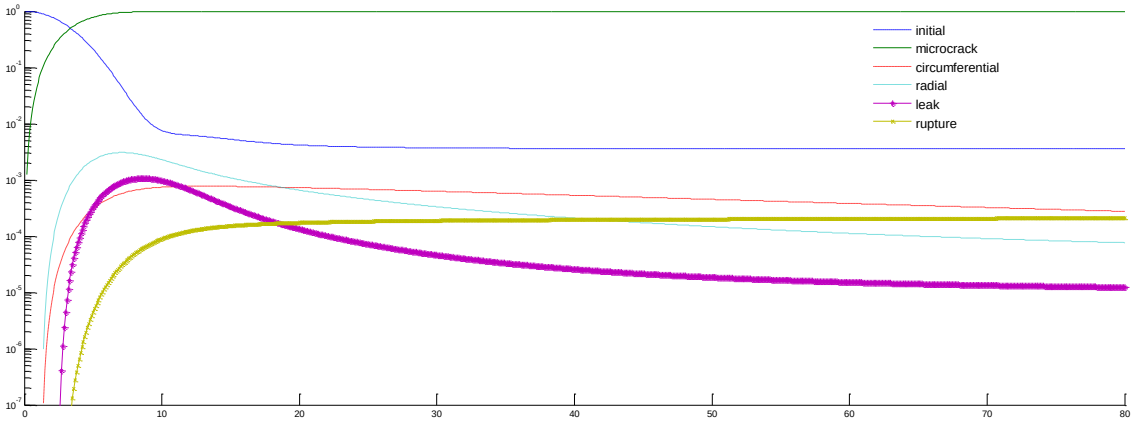

Fig 9. State probabilities obtained by state-space enrichment with step size = 0.1 year.

The numerical comparisons on the state probability values at year 80 are reported in Table II. As expected, the relative differences (i.e. the differences between the state probability values computed by the simulation method minus those obtained with the state-space enrichment method, divided by the former) decrease as the step size is reduced.

Table II
Comparison of simulation results with state-space enrichment results (state probability values at year 80)

	Simulation	State-space enrichment Step size = 1 year	Relative difference	State-space enrichment Step size = 0.5 year	Relative difference	State-space enrichment Step size = 0.1 year	Relative difference
Initial state probability	***0.0036***	0.0033	8.33%	0.0034	5.56%	0.0036	0.00%
Micro-crack probability	***0.9958***	0.9963	-0.05%	0.9961	-0.03%	0.9959	-0.01%
Circumferential crack probability	***2.72e-4***	1.94e-04	28.68%	2.33e-04	14.34%	2.78e-04	-2.21%
Radial crack probability	***7.78e-5***	6.38e-05	17.99%	6.97e-05	10.41%	7.66e-05	1.54%
Leak probability	***1.18e-5***	8.93e-06	24.32%	1.06e-05	10.17%	1.24e-05	-5.08%
Rupture state probability	***2.11e-4***	1.38e-04	34.60%	1.73e-04	18.01%	2.12e-04	-0.47%

All the experiments have been performed in MATLAB on a PC with a 2.1 GH INTEL processor, and a 512 MB memory. The average computation time of the simulation method is 1,069.9 seconds. The computation times of the state-space enrichment method with different time step sizes (e.g. 1 year, 0.5 year, and 0.1 year) are 2.2 seconds, 6.3 seconds, and 290.2 seconds, respectively. The computation expense of the state-space enrichment method increases non-linearly as the time step size decreases. In the current experiments, the simulation method is about 3 times slower than the state-space enrichment method with the time step size 0.1 year. However, it is expected that the state-space enrichment method will be more time consuming when the time step size further decreases, or more degradation states are considered, or a longer time horizon is considered, or any combination of these conditions. This is because such conditions involve a large scale sparse state-space enriched matrix of the dimension $(t_{max} \times (M + 1) \times 1 \Delta t S 2$, where $M+1$ is the total number of degradation states, and $\Delta t S$ is the time step size. Also, the sparse matrix multiplication algorithm has been used in the computation process of state-space enrichment method, because the state-space enriched matrix is close to the size of the memory when Δt_S equals 0.1 year.

5.3 Uncertain external influencing factors

As explained in Section 4, the SPN-supported simulation framework is able to explicitly accommodate the uncertainties in the external influencing factors. To show this ability, as an example, we assign truncated normal distributions to the temperature T and stress σ values of the Weibull scale parameter τ in (15), which is the rate of the first transition. According to [33], τ has the following relationship with temperature and stress.

$$\tau = 9.2 \times 10^{7} \times \sigma^{-7} \times \exp\left(\frac{129}{8.314 \times 10^{-3} \times T}\right)$$

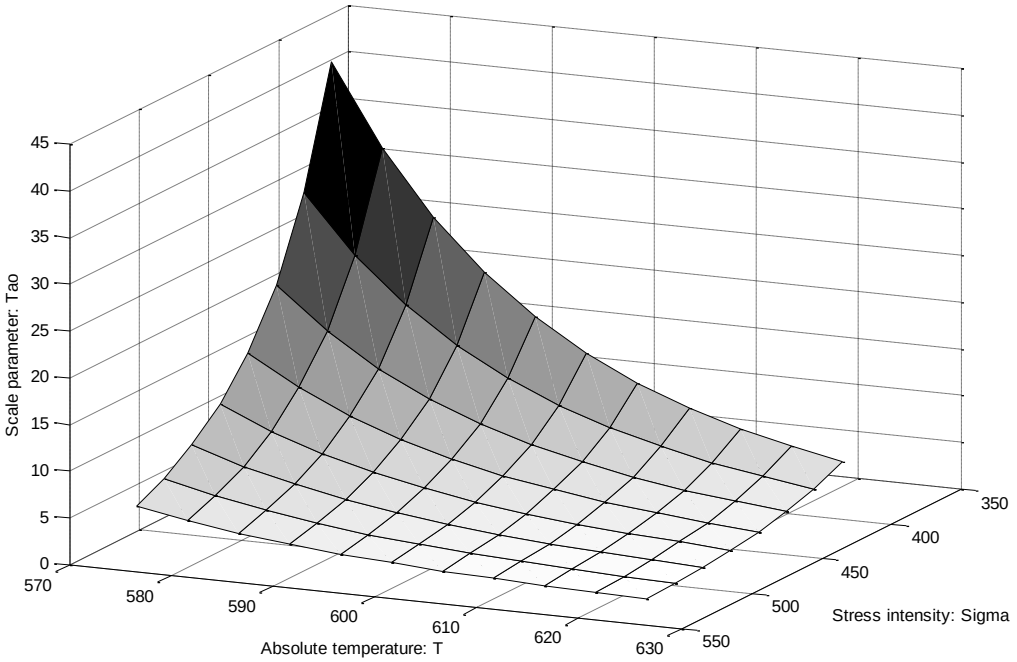

Fig 10. Function of scale parameter τ.

Fig. 10 illustrates the surface plot of τ, given the range [573.15, 623.15] of *T*, and the range [385, 535] of stress σ. These ranges are set to satisfy the maximum limit of τ=40. The truncated normal distributions are defined as

$$p(\sigma) = \frac{\phi(\sigma - 460)}{\phi(535 - 460) - \phi(385 - 460)}$$

$$p(T) = \frac{\phi(T - 598.15)}{\phi(623.15 - 598.15) - \phi(573.15 - 598.15)}$$

where $\phi(\cdot)$ denotes the PDF of a normal distribution. Without loss of generality, the variance is assumed to be 1 for the normal distributions.

The simulation results are displayed in Fig. 12, and Fig. 13 for uncertain temperature, and uncertain stress, respectively, in terms of mean values of the state probabilities (solid lines), together with their 95% confidence intervals (dashed lines). The results in the two Figures appear similar, because from Figure 11 it is seen that the factors *T* and σ have a

similar impact on the values of τ. Additionally, the confidence intervals are larger at lower probability values, which imply a larger variance on rare events.

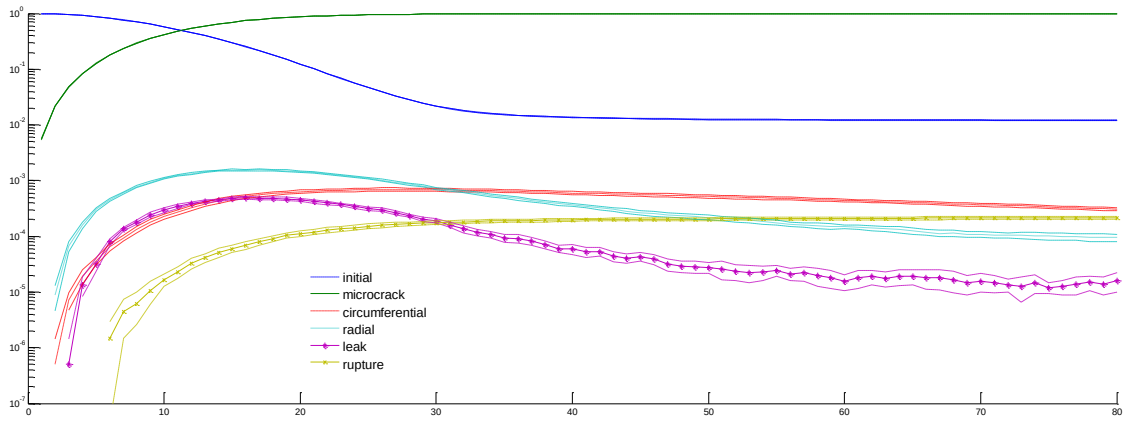

Fig 11. SPN simulation accommodating uncertainty in temperature.

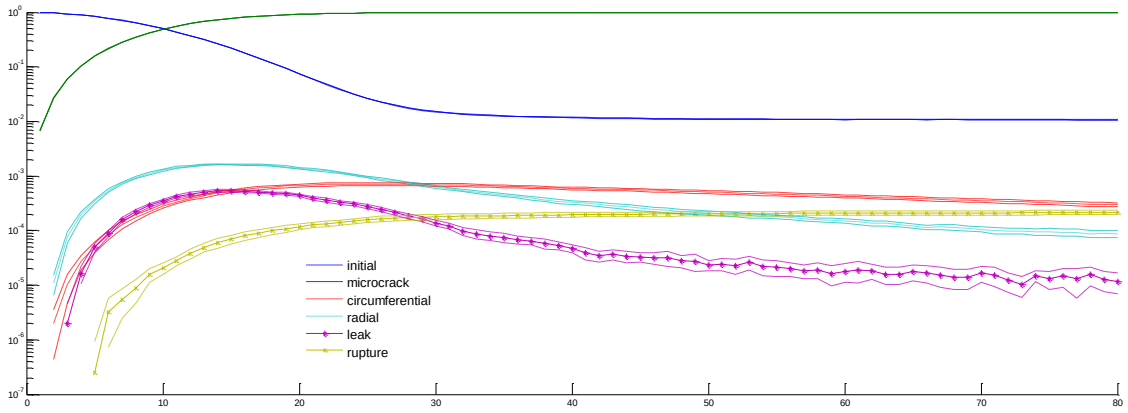

Fig 12. SPN simulation accommodating uncertainty in stress.

Numerical comparisons are reported in Table III and Table IV. Table III gives the mean state probability values at year 80, and the relative differences computed as the percentage differences of the results obtained by simulation with uncertain factors relative to simulation without any uncertain factor. It is observed that both factors have significant impacts on the mean probability value of the initial state, as expected. Table 4 presents the state probability standard deviations averaged over 80 years, and the absolute

relative differences. Both factors have significant impacts on the variability of all state probabilities, especially on initial and micro-crack states, implying that the variances in the uncertain factors influencing the first transition have propagated to the probability estimates of all other states.

Table III
Comparison of simulation results w/o uncertain factors (mean state probability values at year 80)

	Without uncertain factors	Uncertain temperature	Relative differences	Uncertain stress	Relative differences
Initial state probability	***0.0036***	0.012	-236.17%	0.011	-196.79%
Micro crack probability	***0.9958***	0.9873	0.86%	0.9887	0.71%
Circumferential crack probability	***2.72e-4***	2.96e-4	-8.82%	3.04e-4	-11.76%
Radial crack probability	***7.78e-5***	9.15e-5	-17.61%	8.35e-5	-7.33%
Leak probability	***1.18e-5***	1.55e-5	-31.36%	1.35e-5	-14.41%
Rupture state probability	***2.07e-4***	2.14e-4	-3.38%	2.15e-4	-3.62%

Table IV Comparisons of simulation results w/o the uncertain factors (state probability standard deviations averaged over 80 years)

	Without uncertain factors	Uncertain temperature	Absolute relative differences	Uncertain stress	Absolute relative differences
Initial state probability	***1.15e-4***	3.82e-4	230.79%	3.96e-4	242.92%
Micro crack probability	***1.32e-4***	3.87e-4	193.91%	3.93e-4	198.80%
Circumferential crack probability	***2.72e-5***	3.94e-5	45.18%	4.45e-5	63.76%
Radial crack probability	***2.42e-5***	4.10e-5	69.63%	4.16e-5	71.93%
Leak probability	***1.09e-5***	1.92e-5	77.16%	2.01e-5	84.80%
Rupture state probability	***1.70e-5***	2.21e-5	30.18%	2.65e-5	56.13%

6. Conclusions, and future works

An SPN-supported simulation framework has been proposed to solve the multi-state physics model (MSPM) describing a component degradation process with time-dependent transition rates, and uncertain external influencing factors. SPN provides a flexible tool for representing the dynamics of degradation processes, and the simulation solution allows handling time-dependent transition rates and uncertain influencing factors, without complications.

The framework has been applied with success on a nuclear component undergoing stress corrosion cracking. The comparison with analytical approximated results has been satisfactory. The framework has been shown to be capable of indeed explicitly accommodating the uncertainties in the external influencing factors. Thanks to the local place and parallelism of Petri Nets, and the flexibility of Monte Carlo simulation, the

proposed framework has the potential to model the degradation processes of more complex components and systems (e.g. with a larger number of degradation states and transitions), which could be difficult to handle with analytical approximations (e.g. state-space enrichment method).

Future research work is envisaged: 1) comparison with the U.S. Nuclear Regulatory Commission xLPR program [34]; 2) representation and propagation of uncertainty in the external influencing factors when there are insufficient data to assign probabilities (non-probabilistic approaches, e.g. based on Dempster-Shafer theory, would be useful in this respect); 3) extension to more complicated application cases, e.g. including multiple competing degradation processes of components and systems, and interdependencies among the external factors.

Acknowledgement

The authors would like to thank Mr. Mithlesh Kumar for the initial fruitful discussions during his stage work with the Chair on Systems Science and the Energetic Challenge, European Foundation for New Energy-Electricite' de France, at Ecole Centrale Paris, France.

Reference:

[1] Park, C. and Padgett, W. J., "Stochastic degradation models with several accelerating variables " *IEEE Transactions on Reliability,* vol. 55, pp. 379-390, 2006.

[2] Nicolai, R. P., Dekker, R., and Van Noortwijk, J. M., "A comparison of models for measurable deterioration: an application to coatings on steel structures," *Reliability Engineering & System Safety,* vol. 92, pp. 1635-1650, 2007.

[3] Li, W. J. and Pham, H., "Reliability modeling of multi-state degraded systems with multi-competing failures and random shocks," *IEEE Transactions on Reliability,* vol. 54, pp. 297-303, 2005.

[4] Ng, T. S., "An Application of the EM Algorithm to Degradation Modeling," *IEEE Transactions on Reliability,* vol. 57, pp. 2-13, 2008.

[5] Hosseini, M. M., Kerr, R. M., and Randall, R. B., "An inspection model with minimal and major maintenance for a system with deterioration and Poisson failures," *IEEE Transactions on Reliability,* vol. 49, pp. 88-98, 2000.

[6] Zio, E. and Zoia, A., "Parameter Identification in Degradation Modeling by Reversible-Jump Markov Chain Monte Carlo " *IEEE Transactions on Reliability,* vol. 58, pp. 123-131, 2009.

[7] Gebraeel, N., Elwany, A., and Pan, J., "Residual Life Predictions in the Absence of Prior Degradation Knowledge," *IEEE Transactions on Reliability,* vol. 58, pp. 106-117, 2009.
[8] Lawless, J. and Crowder, M., "Covariates and random effects in a gamma process model with application to degradation and failure," *Lifetime Data Analysis,* vol. 10, pp. 213-227, 2004.
[9] Elsayed, E. A. and Liao, H. T., "A geometric Brownian motion model for field degradation data," *International Journal of Materials and Product Technology* vol. 20, pp. 51-72, 2004.
[10] Chryssaphinou, O., Limnios, N., and Malefaki, S., "Multi-State Reliability Systems Under Discrete Time Semi-Markovian Hypothesis," *IEEE Transactions on Reliability,* vol. 60, pp. 80-87, 2011.
[11] Barata, J., Guedes Soares, C., Marseguerra, M., and Zio, E., "Simulation modelling of repairable multi-component deteriorating systems for 'on condition' maintenance optimisation," *Reliability Engineering & System Safety,* vol. 76, pp. 255-264, 2002.
[12] Lisnianski, A. and Levitin, G., *Multi-state System Reliability: Assessment, Optimization and Applications*. Singapore: World Scientific, 2003.
[13] Kuo, W. and Zuo, M. J., *Optimal Reliability Modeling: Principles and Applications*. New York: John Wiley & Sons, 2003.
[14] Chana, G. K. and Asgarpoor, S., "Optimum maintenance policy with Markov processes," *Electric Power Systems Research,* vol. 76, pp. 452-456, 2006.
[15] Sim, S. H. and Endrenyi, J., "A failure-repair model with minimal and major maintenance," *IEEE Transactions on Reliability,* vol. 42, pp. 134-139, 1993.
[16] Black, M., Brint, A. T., and Brailsford, J. R., "A semi-Markov approach for modelling asset deterioration," *Journal of the Operational Research Society,* vol. 56, pp. 1241-1249, 2005.
[17] Kim, J. and Makis, V., "Optimal maintenance policy for a multi-state deteriorating system with two types of failures under general repair," *Computers & Industrial Engineering,* vol. 57, pp. 298-303, 2009.
[18] Liu, Y. and Huang, H. Z., "Optimal Replacement Policy for Multi-State System under Imperfect Maintenance," *IEEE Transactions on Reliability,* vol. 59, pp. 483-495, 2010.
[19] Liu, Y. and Kapur, K. C., "New model and measurement for reliability of multi-state systems," in *Handbook of Performability Engineering*, ed London: Springer, 2008.
[20] Institute, E. P. R., "Materials Reliability Program Crack Growth Rates for Evaluating Primary Water Stress Corrosion Cracking of Alloy 82,182, and 132 Welds," Palo Alto, CA2003.
[21] Unwin, S. D., Lowry, P. P., Layton, R. F., Heasler, P. G., and Toloczko, M. B., "Multi-state physics models of aging passive components in probabilistic risk assessment," in *Proceedings of ANS PSA 2011 International Topical Meeting on Probabilistic Safety Assessment and Analysis*, 2011, pp. 1-12.
[22] Lisnianski, A., Frenkel, I., Khvatskin, L., and Ding, Y., "Maintenance contract assessment for aging systems," *Quality & Reliability Engineering International,* vol. 24, pp. 519-531, 2008.
[23] Petri, C. A., "Communication with automation," Rome Air Development Center, Griffis (NY)1966.
[24] Yang, N. H., Yu, Y. Q., Qian, Z. L., and Sun, H., "Modeling and quantitatively predicting software security based on stochastic Petri nets," *Mathematical and Computer Modelling,* vol. In press, 2011.

[25] Kleyner, A. and Volovoi, V., "Application of Petri nets to reliability prediction of occupant safety systems with partial detection and repair," *Reliability Engineering & System Safety,* vol. 95, pp. 506-613, 2010.
[26] Schneeweiss, W. G., "Tutorial: Petri nets as a graphical description medium for many reliability scenarios," *IEEE Transactions on Reliability,* vol. 51, pp. 39-48, 2002.
[27] Reisig, W., "Petri nets with individual tokens," *Theoretical Computer Science,* vol. 41, pp. 185-213, 1985.
[28] Trivedi, S. K., *Probability and statistics with reliability, queuing and computer science applications*, 2nd ed.: John Wiley and Sons, 2002.
[29] Dutuit, Y., Chatelet, E., Signoret, J. P., and Thomas, P., "Dependability modeling and evaluation by using stochastic Petri nets: application to two test cases.," *Reliability Engineering & System Safety,* vol. 55, pp. 117-124, 1997.
[30] Lewis, E. E. and Tu, Z. G., "Monte Carlo reliability modeling by inhomogeneous Markov processes," *Reliability engineering,* vol. 16, pp. 277-296, 1986.
[31] Rubinstein, R. Y. and Kroese, D. P., *Simulation and the Monte Carlo Method*, 2nd ed.: Wiley, 2009.
[32] Fleming, K. N., Unwin, S. D., Kelly, D., Lowry, P. P., Toloczko, M. B., Layton, R. F., Youngblood, R., Collins, D., Huzurbazar, A. V., Williams, B., and Heasler, P. G., "Treatment of Passive Component Reliability in Risk-Informed Safety Margin Characterization," Idaho National Laboratory, INL/EXT-10-20013, Idaho Falls, Idaho2010, pp. 1-210.
[33] Aly, O. F., "Preliminary Study for Extension and Improvement on Modeling of Primary Water Stress Corrosion Cracking at Control Rod Drive Mechanism Nozzles of Pressurized Water Reactors," in *International Nuclear Atlantic Conference (INAC)*, Rio de Janeiro, 2009.
[34] Mattie, P. D., Kalinich, D. A., and Sallaberry, C. J., "U.S. Nuclear Regulatory Commission Extremely Low Probability of Rupture Pilot Study: xLPR Framework Model User's Guide," Sandia National Laboratories, SAND2010-7131, Albuquerque, New Mexico and Livermore, California2010.

Yan-Fu Li (M'11) is an Assistant Professor at Ecole Centrale Paris (ECP) & Ecole Superieure d'Electricite (SUPELEC), Paris, France. Dr. Li completed his PhD research in 2009 at National University of Singapore, and went to the University of Tennessee as a research associate. His research interests include reliability and safety modeling, Monte Carlo simulation, and artificial intelligence. He is the author of more than 20

publications, all in refereed international journals, conferences, and books. He is an invited reviewer of 9 international journals. He is a member of the IEEE.

Enrico Zio (M'06–SM'09) has a B.S. in nuclear engineering, Politecnico diMilano,1991; a M.Sc. in mechanical engng., UCLA, 1995; a Ph.D., in nuclear engng.,Politecnico di Milano, 1995; and a Ph.D., in nuclear engng., MIT, 1998. He is the Director of the Graduate School of the Politecnico di Milano, and the full Professor of Computational Methods for Safety and Risk Analysis. He is the Chairman of the European Safety and Reliability Association, ESRA. He is a member of the editorial board of various international sciatic journals on reliability engineering and system safety. He is co-author of four international books, and more than 170 papers in international journals. He serves as referee of several international journals.

Yan-Hui Lin is a master student at Ecole Centrale Paris (ECP, Paris, France) & Ecole Centrale de Pékin (Beihang University, Beijing, China). His research interests are in simulation, reliability, and safety modeling.